Am J Physiol Regul Integr Comp Physiol 311: R582–R591, 2016.
First published July 20, 2016; doi:10.1152/ajpregu.00180.2016.

Highly sensitive index of sympathetic activity based on time-frequency spectral analysis of electrodermal activity

Hugo F. Posada-Quintero,[1] John P. Florian,[2] Álvaro D. Orjuela-Cañón,[3] and Ki H. Chon[1]

[1]*University of Connecticut, Storrs, Connecticut;* [2]*Navy Experimental Diving Unit, Panama City, Florida; and* [3]*Universidad Antonio Nariño, Bogotá, Colombia*

Submitted 2 May 2016; accepted in final form 14 July 2016

Posada-Quintero HF, Florian JP, Orjuela-Cañón AD, Chon KH. Highly sensitive index of sympathetic activity based on time-frequency spectral analysis of electrodermal activity. *Am J Physiol Regul Integr Comp Physiol* 311: R582–R591, 2016. First published July 20, 2016; doi:10.1152/ajpregu.00180.2016.—Time-domain indices of electrodermal activity (EDA) have been used as a marker of sympathetic tone. However, they often show high variation between subjects and low consistency, which has precluded their general use as a marker of sympathetic tone. To examine whether power spectral density analysis of EDA can provide more consistent results, we recently performed a variety of sympathetic tone-evoking experiments (43). We found significant increase in the spectral power in the frequency range of 0.045 to 0.25 Hz when sympathetic tone-evoking stimuli were induced. The sympathetic tone assessed by the power spectral density of EDA was found to have lower variation and more sensitivity for certain, but not all, stimuli compared with the time-domain analysis of EDA. We surmise that this lack of sensitivity in certain sympathetic tone-inducing conditions with time-invariant spectral analysis of EDA may lie in its inability to characterize time-varying dynamics of the sympathetic tone. To overcome the disadvantages of time-domain and time-invariant power spectral indices of EDA, we developed a highly sensitive index of sympathetic tone, based on time-frequency analysis of EDA signals. Its efficacy was tested using experiments designed to elicit sympathetic dynamics. Twelve subjects underwent four tests known to elicit sympathetic tone arousal: cold pressor, tilt table, stand test, and the Stroop task. We hypothesize that a more sensitive measure of sympathetic control can be developed using time-varying spectral analysis. Variable frequency complex demodulation, a recently developed technique for time-frequency analysis, was used to obtain spectral amplitudes associated with EDA. We found that the time-varying spectral frequency band 0.08–0.24 Hz was most responsive to stimulation. Spectral power for frequencies higher than 0.24 Hz were determined to be not related to the sympathetic dynamics because they comprised less than 5% of the total power. The mean value of time-varying spectral amplitudes in the frequency band 0.08–0.24 Hz were used as the index of sympathetic tone, termed TVSymp. TVSymp was found to be overall the most sensitive to the stimuli, as evidenced by a low coefficient of variation (0.54), and higher consistency (intra-class correlation, 0.96) and sensitivity (Youden's index > 0.75), area under the receiver operating characteristic (ROC) curve (>0.8, accuracy $>$ 0.88) compared with time-domain and time-invariant spectral indices, including heart rate variability.

electrodermal activity; sympathetic function; autonomic nervous system; variable frequency complex demodulation; stand test; cold pressor; tilt table test

SENSITIVE MEASURES OF SYMPATHETIC tone are needed because of the prevalence of sympathetic control impairment in certain cardiovascular diseases and pathophysiological conditions (8, 23). In many cardiovascular diseases, sympathetic control impairment is a factor either in the development or in the progression of the pathological process (15, 47). While there are various approaches to measuring sympathetic function, the invasiveness of certain techniques, their inability to provide continuous monitoring, or their inaccurate assessment of sympathetic dynamics renders their widespread use impractical (23). In cardiovascular autonomic neuropathy, for example, sympathetic denervation is a marker of the progress of the disease from early to severe stages (16, 36), and the gold standard procedure for sympathetic assessment, the cardiovascular autonomic reflex tests (49a), is found to be insensitive (50%) for this task (52).

A widely used noninvasive means to assess the dynamics of the autonomic nervous system is to compute the power spectral density of heart rate variability (HRV) (54a). The high-frequency components of HRV are known to be solely influenced by the parasympathetic system. In contrast, the low-frequency (0.045–0.15 Hz) components of HRV (HRVLF or HRVLFn when normalized to total power of HRV) are influenced by both the sympathetic and parasympathetic nervous systems. Despite the limitation of also being influenced by parasympathetic activity, HRVLF has been used to assess sympathetic tone (54a).

Electrodermal activity (EDA) is being increasingly used as a surrogate measure of the sympathetic activities (18), as sudomotor activity is known to be solely controlled by the sympathetic nervous system (26, 30, 50). Traditionally, analysis of EDA has been in the time-domain (3), using skin conductance level (SCL) and nonspecific skin conductance responses (NS.SCRs). However, several studies have reported high variability with these time-domain indices (10, 43). Time-invariant frequency-domain analysis of electrodermal activity has recently been reported as a tool for sympathetic tone assessment, and it was termed EDASympn (43). The usefulness of EDASympn was demonstrated, with lower variability compared with time-domain measures of EDA, but the technique exhibited only acceptable consistency, with lower sensitivity for orthostatic (stand test) and cognitive stress compared with SCL and NS.SCRs.

Given that the sympathetic tone is time varying, especially when experiments are specifically designed to invoke its dynamics, we hypothesized that time-varying analysis of EDA may provide more sensitive results than the time-invariant frequency-domain analysis (42) and time-domain indices consisting of SCL and NS.SCRs. To this end, we performed time-frequency analysis of EDA signals to examine whether we can obtain an even more sensitive and reliable index of sympathetic tone. Specifically, variable frequency complex

Address for reprint requests and other correspondence: K. H. Chon, Univ. of Connecticut, 260 Glenbrook Rd., Unit 3247, Storrs, CT 06269-3247 (e-mail: kchon@engr.uconn.edu).

demodulation (VFCDM), a time-frequency spectral (TFS) analysis technique that provides accurate amplitude estimates and one of the highest time-frequency resolutions (7) was employed in this study to develop an index of sympathetic tone. The time-varying EDA index of sympathetic control (TVSymp) was computed by using the mean spectral amplitudes in the frequency band associated with sympathetic tone of the EDA.

To test our hypothesis, we have computed TVSymp and a full set of EDA (SCL, NS.SCRs, and EDASympn) and HRV (HRVLF and HRVLFn) indices of sympathetic control for subjects undergoing four tests known to elicit sympathetic tone arousal: cold pressor test, 70° head-up tilt (HUT) test, stand test, and the Stroop task. Sensitivity, consistency, and variability of TVSymp were computed and compared against the time-domain and time-invariant spectral indices.

MATERIALS AND METHODS

Protocol

Participants were asked to avoid caffeine and alcohol and to not exercise during the 24 h preceding the test and were instructed to fast for at least 3 h before testing. Prospective subjects using psychoactive drugs, nicotine, or other recreational drugs, and taking any medicine were asked to exclude themselves from the study. The experiments were carried out in a quiet, dimly lit room (ambient temperature, 26–27°C). The study protocol was approved by the Institutional Review Board of the University of Connecticut, and all volunteers provided written informed consent to participate in the experiment. ECG and EDA signals were simultaneously recorded throughout all of the tests (Hewlett-Packard HP 78354A and ADINSTRUMENTS GSR module, respectively). After preparing the skin with alcohol, ECG electrodes were placed to acquire Lead I, and EDA electrodes were placed on the index and middle finger for all subjects. Signals were digitized using a PowerLab system at 1 kHz, with 12-bit resolution.

Twelve healthy volunteers (10 males, 2 females) of ages ranging from 19 to 36 yr old (26.2 ± 6.1; mean ± SD), weight 64.6 ± 7 kg, and height 171.5 ± 9.6 cm, were enrolled in this study. No gender-related differences have been reported for EDA or sympathetic function. To induce a wide variety of sympathetic arousal types, subjects underwent four tests, in the following order: cold pressor (physical stress), 70° HUT, stand test (orthostatic stress), and the Stroop task (cognitive stress). The order of tests was the same for all of the subjects.

Before each test, subjects remained in the supine position for at least 5 min to ensure hemodynamic stabilization (end-point criteria was when the subject achieved a baseline level of heart rates). After the stabilization period, 5 min of resting baseline data were recorded with subjects in the supine position before each test. For the cold pressor test, subjects were asked to immerse their left hand to the wrist level into a 0–1°C water bath for a period of 3 min. For HUT, subjects were tilted from 0 to 70° and remained tilted for 5 min. The stand test consisted of a 5-min standing period in which subjects were asked not to move and not to actively contract their leg muscles. For the Stroop task, subjects were asked to say a word that named a color. They were shown congruent (the word was written in the color it expressed) and incongruent (the word and the color it was printed in were different) combinations to induce cognitive stress (53). The words and colors were "blue," "yellow," "green," "red," "purple," and "black". The background also changed to be randomly congruently or incongruently colored with the word. A computerized version of the original Stroop task was designed. The Stroop task was 5 min total, with the first minute used for training.

Signal Processing

TFS of EDA signals were used to quantify the elicited changes of the sympathetic nervous system due to the cold pressor test, HUT, stand test, and the Stroop task. Prior to time-frequency analysis, EDA signals were down-sampled to 2 Hz and high-pass filtered (0.01 Hz) to remove any trends. The VFCDM technique has been described in detail previously (7, 59) and has been tested with different physiological signals (51, 59, 65); hence, the technique will be only briefly summarized.

Variable frequency complex demodulation algorithm. The first step is to use complex demodulation (CDM) to obtain an estimate of the TFS. In CDM, a bank of low-pass filters (LPFs) is used to decompose the signal into a suite of band-limited signals. The analytic signals that are obtained from these, through the use of the Hilbert transform, then provide estimates of instantaneous amplitude, frequency, and phase within each frequency band. Consider a sinusoidal signal $x(t)$ to be a narrow-band oscillation with a center frequency f_0, instantaneous amplitude $A(t)$, phase $\Phi(t)$, and the direct current component $dc(t)$ defined as

$$x(t) = dc(t) + A(t)\cos\left[2\pi f_0 t + \phi(t)\right] \tag{1}$$

For a given center frequency (or carrier), we can extract the instantaneous amplitude information $A(t)$ and phase information $\Phi(t)$ by multiplying $x(t)$ by $e^{j2\pi f_0 t}$, which results in the following:

$$\begin{aligned} z(t) &= x(t)e^{-j2\pi f_0 t} \\ &= dc(t)e^{-j2\pi f_0 t} + \left[\frac{A(t)}{2}\right]e^{j\phi t} + \left[\frac{A(t)}{2}\right]e^{-j[4\pi f_0 t + \phi(t)]} \end{aligned} \tag{2}$$

A leftward shift by $e^{j2\pi f_0 t}$ moves the center frequency f_0 to zero frequency in the spectrum of $z(t)$. If $z(t)$ is subjected to an ideal LPF with a cutoff frequency $f_C < f_0$, then the filtered signal $z_{1P}(t)$ will contain only the component of interest, and we obtain

$$z_{1P}(t) = \left[\frac{A(t)}{2}\right]e^{j\phi(t)} \tag{3}$$

$$A(t) = 2\left|z_{1P}(t)\right| \tag{4}$$

$$\phi(t) = \tan^{-1}\left\{\frac{\mathrm{Im}\left[z_{1P}(t)\right]}{\mathrm{Re}\left(z_{1P}[t]\right)}\right\} \tag{5}$$

Consider a case when a modulating frequency is not fixed as described before but varies as a function of time. In this case, the signal $x(t)$ can be written in the following form:

$$x(t) = dc(t) + A(t)\left\{\int_0^t \cos\left[2\pi f(\tau)d\tau + \phi(t)\right]\right\} \tag{6}$$

Similar to the operations in *Eqs. 1* and *2*, multiplying *Eq. 6* by $e^{-j\int_0^t 2\pi f(\tau)d\tau}$ yields both instantaneous amplitude, $A(t)$, and instantaneous phase, $\Phi(t)$ (20), so that

$$\begin{aligned} z(t) = x(t)e^{-j\int_0^t 2\pi f(\tau)d\tau} = dc(t)e^{-j\int_0^t 2\pi f(\tau)d\tau} + \frac{A(t)}{2}e^{j\phi(t)} \\ + \frac{A(t)}{2}e^{-j\int_0^t 4\pi f(\tau)d\tau} \end{aligned} \tag{7}$$

From *Eq. 7*, when $z(t)$ is filtered with an ideal LPF with a cutoff frequency $f_C < f_0$, then the filtered signal $z_{1P}(t)$ will be obtained with the same instantaneous amplitude $A(t)$ and phase $\Phi(t)$, as provided in *Eqs. 4* and *5*. The instantaneous frequency, as reported previously (41), is given by

$$f(t) = f_0 + \frac{1}{2\pi}\frac{d\phi(t)}{dt} \tag{8}$$

For this study, $x(t)$ corresponds to the EDA signal. The instantaneous frequency and amplitude of d_i can be calculated using the Hilbert transform (29). The entire time-frequency spectrum can be obtained by the calculation of the Hilbert transform of the equation above for all time points for the obtained low-pass-filtered frequency components. Therefore, by the combination of the CDM and the Hilbert transform, a high time-frequency (TF) resolution spectrum and accurate amplitude information can be obtained.

The procedure for the implementation of the CDM-based TFS is summarized next.

1. Design a finite-impulse response (FIR) LPF with the bandwidth and the length of the filter set to F_ω and N_ω, respectively. Set center frequencies as

$$f_{0i} = (i-1)(2F_\omega), \quad i = 1, 2, \ldots, \ \text{int}\left(\frac{f_{\max}}{2F_\omega}\right) \tag{9}$$

where the bandwidth between neighboring center frequencies is $2F\omega$, and $f_{\max}$ represents the highest signal frequency.

2. Use the CDM to extract the dominant frequency within the confined bandwidth and repeat it over the entire frequency band (by incrementing f_{0i}).

3. Decompose the signal into sinusoidal modulations via the CDM.

4. Calculate the instantaneous frequencies using *Eq. 8* based on the phase (*Eq. 5*) and the instantaneous amplitudes (*Eq. 4*) of each sinusoidal modulation component using the Hilbert transform.

5. Obtain the TF representation of the signal using the estimated instantaneous frequencies and amplitudes.

Determining the relevant components for the sympathetic responses. Once the TFS is obtained via the VFCDM method as described above (e.g., Fig. 1), the resulting time-varying spectral amplitudes at each frequency interval are analyzed to examine whether they evolve in time in response to sympathetic stimulation. These spectral amplitudes are not rigid bands of frequency. Instead, they represent the evolution over time of a spectral amplitude that changes within a range of frequencies (see Fig. 2). These frequencies depend on the sampling frequency (fs) and given that fs = 2 Hz was selected, the spectral frequencies are centered on 0.04, 0.12, 0.2, 0.28, 0.36, 0.44, 0.52, 0.6, 0.68, 0.76, 0.84, and 0.92 Hz. Finer spectral resolution was explored. Because we were only interested in the sum of time-varying spectral amplitudes in the frequency range that may correspond to the sympathetic dynamics (e.g., 0.045–0.25 Hz), finer frequency resolution was not found informative.

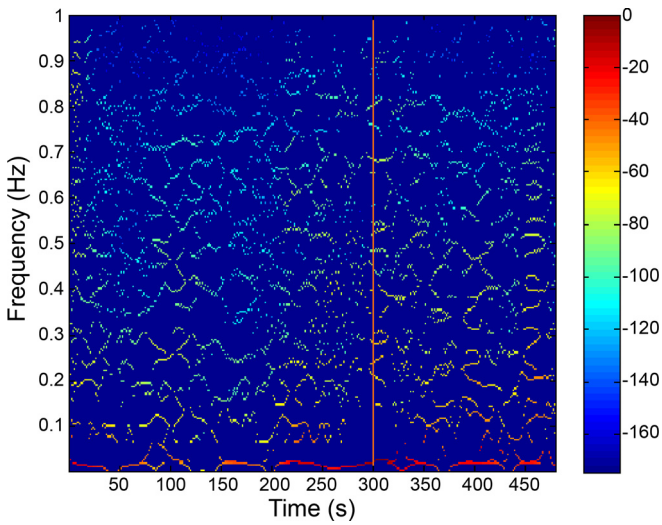

Fig. 1. Normalized amplitude time-frequency spectrum of an electrodermal activity (EDA) signal, obtained via the complex demodulation method (variable frequency complex demodulation, or VFCDM), for a given subject under the cold pressor test. Vertical line represents the start of the cold pressor. Color bar shows the logarithmic scale.

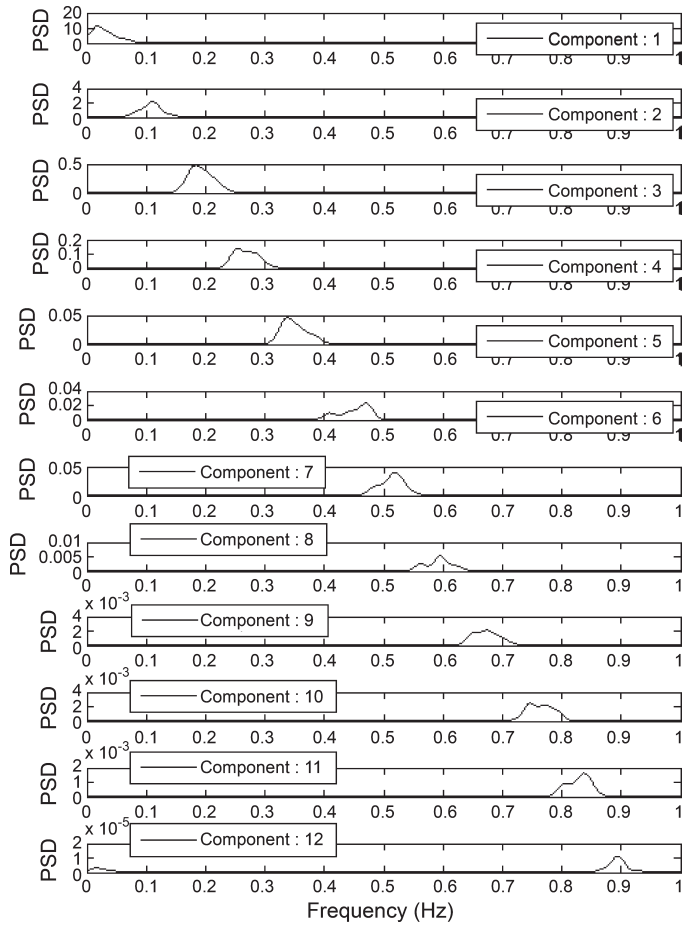

Fig. 2. Exemplification of the 12 resulting VFCDM components, shown in frequency domain. Sampling frequency is 2 Hz.

The power contained in each frequency resolution band was computed for all subjects to determine sympathetic tone-relevant dynamics. Those powers that did not change from baseline to stimuli stage were considered insensitive to sympathetic control and subsequently considered irrelevant. The time-varying spectral powers with a low value (comprising less than 5% of the total spectral power) were also considered irrelevant. It was recently shown that ~5% of time-invariant spectral content of HRV is also enclosed in frequencies above HF (>0.4 Hz) (43). In the same study, the frequency bound of EDA associated with the sympathetic activity was largely confined to 0.045 to 0.25 Hz, with about 5% of the power in the frequencies beyond 0.25 Hz (42).

Computing the index of sympathetic control. Time-varying spectral amplitudes in the frequency bands that are considered to be responsive to sympathetic stimuli are summed together to obtain an estimated reconstructed EDA signal [$X'(t)$], which is then normalized to unit variance (divided by its standard deviation), and its instantaneous amplitude is computed using the Hilbert transform (29), as follows

$$Y'(t) = \frac{1}{\pi} P \int_{-\infty}^{\infty} \frac{X'(\tau)}{t-\tau} d\tau \tag{10}$$

where P indicates the Cauchy principal value. $X'(t)$ and $Y'(t)$ form the complex conjugate pair, so we can define an analytic signal, $Z(t)$, as

$$Z(t) = X'(t) + iY'(t) = a(t)e^{j\theta(t)} \tag{11}$$

in which

$$a(t) = \left[X'^2(t) + Y'^2(t)\right]^{1/2},\ \theta(t) = \arctan\left(\frac{Y'(t)}{Y'(t)}\right). \quad (12)$$

The resulting $a(t)$ is considered the instantaneous amplitude of $Z(t)$ (see Fig. 3). The mean amplitude of $a(t)$, termed TVSymp, was computed for the four tests for all subjects. This value constitutes our intended index of sympathetic tone. Notice that TVSymp is a dimensionless quantity, as it was normalized to the standard deviation.

EDA indices. To extract the conductance level of EDA, a 10th-order low-pass FIR filter with a cut-off frequency of 0.0004 Hz was applied. The raw signal minus the conductance level was used to compute the NS.SCRs. The SCL index was computed using the mean of the conductance level over the 2-min period. NS.SCRs were obtained by visual inspection over the 2-min period, and averaged per minute. A threshold value of 0.05 μS was used to determine relevant SCRs (3). In addition, when a second response occurred before completion of the prior response, the two responses were counted as two NS.SCRs, even though they were overlapped.

The time-invariant frequency domain index of EDA, EDASympn, was also computed. Power spectral density analysis of EDA signals was performed on the same 2-min segments used to compute SCL and NS.SCRs. For this process, EDA signals were down-sampled to 2 Hz. Before down-sampling, the data were filtered with an 8th-order Chebyshev Type I low-pass filter (0.8 Hz). Down-sampling from 400 Hz to 2 Hz was performed in two steps (using consecutive down-sampling factors of 1/20 and 1/10, respectively). Finally, signals were high-pass filtered (0.01 Hz, Butterworth, 8th order) to remove any trend. The power spectra of EDA signals were calculated using Welch's periodogram method with 50% data overlap. A Blackman window (length of 128 points) was applied to each segment, the fast Fourier transform was calculated for each windowed segment, and the power spectra of the segments were averaged. EDASympn was computed as the normalized power within the frequency band of interest (0.045 to 0.25 Hz) (43).

HRV analysis. For HRV analysis, ECG signals were band-pass filtered (0.05–40 Hz) to reduce noise and motion artifacts. The R-waveform peaks were detected using a widely used peak detection algorithm (57), and HRV series (from RR segments) were computed. The power spectra of HRV were calculated using Welch's periodogram method with 50% data overlap. The R-R interval series were converted to an evenly time-sampled signal (4 Hz) by cubic spline interpolation. A Blackman window (length of 256 points) was applied to each segment, and the fast Fourier transform was calculated for each windowed segment. Finally, the power spectra of the segments were averaged. The low-frequency index [HRVLF [ms^2], 0.04 to 0.15 Hz] (54a) and normalized LF index [HRVLFn = (HRVLF)/Total power, normalized units] were computed. Four minutes of clean ECG signals were used to compute HRV for HUT, the stand test, and the Stroop task, and 3 min for the cold pressor test given the extreme characteristics of this physical test. Within each test, the same data length was used consistently for baseline and test segments.

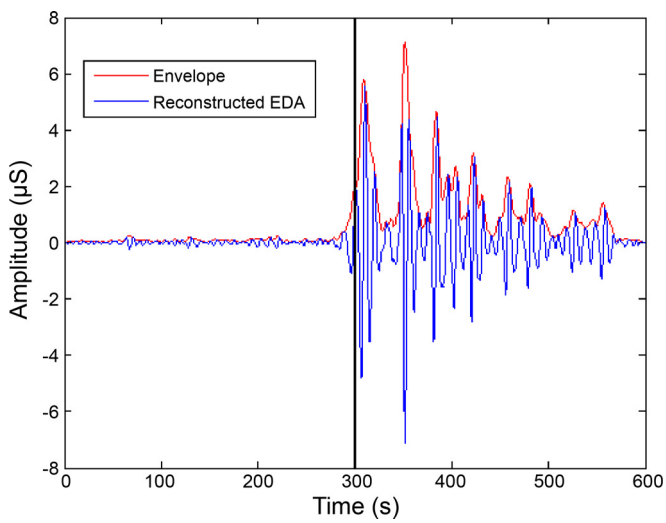

Fig. 3. Computed envelope for the sum of selected VFCDM backbones, for a given subject, during the stand test. The blue line is the reconstructed signal using the two components with the most power. The red line represents the envelope, estimated via instantaneous amplitude. Vertical black line represents the moment when the subject stood up.

Statistics. Six indices of sympathetic control were computed, including one time-frequency domain index, TVSymp, two time-domain indices, SCL (μS), and NS.SCRs (no./min), and three frequency-domain indices, EDASympn (normalized units, n.u.), HRVLF (ms^2), and HRVLFn (n.u.). All of the statistical analysis was performed using MATLAB. The paired t-test was applied to test the null hypothesis that elicited responses to the cold pressor test, HUT testing, the stand test, and the Stroop task, as measured by each of the above-defined indices, are equal to the baseline values. A P value <0.05 was set to define statistical significance. These results are useful to evaluate the suitability of the indices to quantitatively assess sympathetic function in healthy subjects.

Measures from detection theory analysis were employed to assess sensitivity of the indices, including the ROC curve (39), Youden's index (J = Sensitivity + Specificity − 1, to assess the performance of the detector) (62), the area under the ROC curve [area under the curve (AUC), the probability that the index will assign to a positive instance a higher value than to a negative one] (25), and the maximum accuracy of the detector. The coefficient of variation (CV) (i.e., the standard deviation between all of the measurements divided by the mean) and the intraclass correlation (38) were computed for all of the indices to assess intersubject variability and degree of consistency of each index, respectively.

RESULTS

Figure 2 illustrates how the time-varying spectral powers are distributed in the frequency domain. Notice how as frequency increases, the power decreases (note that y-axes are not equal). Table 1 shows the percentage of spectral power contained in three bands of frequencies throughout the subjects. The time-varying spectral amplitudes in the first band comprise most of the spectral content of the signal (>60%) for any test. The percentage of spectral power at the very low frequencies (<0.08 Hz) is usually reduced under testing conditions compared with the baseline, because sympathetic dynamics become more pronounced with test stimuli (43). Time-varying spectral components at frequencies between 0.08 and 0.24 Hz (2nd and 3rd center frequencies) are the ones that bear the most power and increase the most between baseline and tests. Although some of the remaining spectral power increased during testing at >0.24 Hz, it was less than 5% of the power. For this reason, we have selected the spectral amplitudes in the 0.08 to 0.24 Hz range to compute the sympathetic index.

Table 2 shows the overall EDA and HRV response for the cold pressor test, HUT, stand test, and the Stroop task, along with the significance of differences found between baseline and stimuli for each index. All EDA measures (TVSymp, SCL, NS.SCRs, and EDASympn) significantly increased between baseline and test stages. HRVLF only exhibited significant differences during the stand test and the Stroop task. HRVLFn showed differences during HUT and the stand test, but not during cold pressor or the Stroop task. Figure 4 shows 8 min (6 min in the case of cold pressor as this test was shorter) of time

Table 1. *Percentage of power for the resulting backbones of VFCDM*

	Cold Pressor		70° Head-up Tilt		Stand Test		Stroop Task	
Frequency Range	Baseline	Test	Baseline	Test	Baseline	Test	Baseline	Test
0 to 0.08 Hz	88.3	67.7	86	83.8	91.1	81.8	89.4	81
0.08 to 0.24 Hz	6.9	19.5	8.4	7.5	5.4	10	6.5	11.4
0.24 to 1 Hz	2.2	4.3	1.7	2.9	0.7	1.9	2.2	2.3

Values are % of total power throughout the full set of subjects.

evolution (means ± SD) of TVSymp for cold pressor, HUT, stand test, and the Stroop task. For all stimuli, TVSymp reaches a maximum value at ~2 min and then gradually decreases with time. However, the Stroop task differs from other stimuli in that the maximum values linger for long time durations and then gradually decrease to baseline values. Note that before each test, subjects remained in the supine position for at least 5 min to ensure hemodynamics stabilization. This can be seen in Table 2 especially for TVSymp, as its baseline values are nearly identical prior to stimuli.

Results for the analysis of sensitivity are shown in Table 3. TVSymp outperformed all the other indices (highest J) at detecting stress, with the only exception being HRVLFn, which exhibited a higher performance ($J = 1$ vs. $J = 0.83$) during the stand test. NS.SCRs and TVSymp exhibited equal J values for the stand test. TVSymp also showed a higher probability to assign a higher value to a positive instance than to a negative one (highest AUC). NS.SCRs and HRVLFn equaled TVSymp on this measure for the Stroop task and postural stimulation (stand test), respectively. Similar behavior was found for the accuracy, where TVSymp surpassed all the other indices, with the only exception being HRVLFn during the stand test (Acc = 1 vs. Acc = 0.92). Figure 5 includes ROC curves for the four tests. Notice how the TVSymp ROC curve is more pronounced toward the left top corner, with the only exception being the stand test curve, where HRVLFn curve is slightly higher.

As for the measures of variation and consistency, Table 4 shows how TVSymp exhibits higher variation during baseline, compared with the four tests. However, such variation is almost always lower than the variation of SCL and NS.SCRs. NS.SCRs were only less variable during the stand test baseline. That is consistent with studies that report high variability of SCL and NS.SCRs, a concern among researchers (10), impeding the widespread use of these indices for assessing the general state of activation of the sympathetic system. Compared with EDASympn, TVSymp exhibited similar CV, slightly lower for cold pressor and HUT, and higher for the stand test and the Stroop task baselines. HRVLF was one of the more variable indices, ranking third overall after SCL and NS.SCRs. In contrast, HRVLFn was the least variable index overall.

TVSymp was the most consistent index, as its intraclass correlation achieved a very high value of 0.96 with bounds between 0.9 and 0.99 for a level of significance of 0.05. Even though SCL's and NS.SCRs' consistencies were high, in agreement with previously reported values (43), their consistencies were not as high as those of TVSymp. The least consistent index was the EDASympn. HRVLF and HRVLFn proved to be moderately consistent indices.

DISCUSSION

The time-varying spectral EDA index of sympathetic control, TVSymp, was significantly higher during the cold pressor test, HUT, stand test, and the Stroop task, compared with baseline. TVSymp can be used as a noninvasive measure for assessing sympathetic function, as these induced stressors are known to invoke the sympathetic nervous system's response. Measures of detection theory showed that TVSymp is the most sensitive index of sympathetic arousal overall for the four stimuli experiments in the study, with the exception of the stand test, where HRVLFn was slightly better. Furthermore, TVSymp exhibited lower variability (coefficient of variation) than did time-domain EDA indices (SCL and NS.SCRs), and higher consistency (intra-class correlation coefficient) than any other tested index of sympathetic control. Time-frequency analysis of EDA provides relevant information about sympathetic arousal in different scenarios, as all biological systems are time-variant, increasing the potential for an EDA signal to be used for detecting the onset and level of stress induced by various stimuli. However, more testing is needed to determine the method to be applied to diagnose the onset and progression of diseases that affect the autonomic nervous system.

Traditionally, techniques for sympathetic function assessment have involved hemodynamic measurements (5, 55), ad-

Table 2. *Results for EDA and HRV indices*

Index	Stage	Cold Pressor	70° Head-up Tilt	Stand Test	Stroop Task
TVSymp	Baseline	0.5 ± 0.3	0.3 ± 0.3	0.3 ± 0.3	0.2 ± 0.3
	Test	1.4 ± 0.7*	1.6 ± 0.7*	1.6 ± 0.7*	1.4 ± 0.7*
SCL, μS	Baseline	0.8 ± 4.7	2.9 ± 6.2	4.1 ± 8.1	−1.3 ± 3.9
	Test	4.5 ± 7.5*	6.5 ± 8.4*	10.8 ± 7.5*	6.3 ± 4.0*
NS.SCR, no./min	Baseline	2.7 ± 2.9	1.5 ± 2.3	1.8 ± 2	0.9 ± 1.5
	Test	4.9 ± 4.5*	3.6 ± 2.7*	6 ± 2.9*	9.8 ± 3.9*
EDASympn, n.u.	Baseline	0.2 ± 0.2	0.2 ± 0.2	0.3 ± 0.2	0.3 ± 0.2
	Test	0.4 ± 0.2*	0.4 ± 0.2*	0.5 ± 0.2*	0.5 ± 0.2*
HRVLF, ms^2	Baseline	7.1 ± 6.4	4.7 ± 3.9	3.8 ± 3.9	4.2 ± 3.4
	Test	4.8 ± 3.3	16 ± 21	36 ± 33*	6.1 ± 4.4*
HRVLFn, n.u.	Baseline	0.3 ± 0.1	0.3 ± 0.1	0.2 ± 0.05	0.4 ± 0.1
	Test	0.3 ± 0.1	0.5 ± 0.2*	0.6 ± 0.2*	0.4 ± 0.1

Values are expressed as means ± SD. *Significant difference compared to baseline stage ($P < 0.05$). TVSymp, time-varying index of sympathetic tone; SCL, skin conductance level; NS.SCRs, nonspecific skin conductance responses; EDASympn, normalized sympathetic component of the EDA; HRVLF, low-frequency components of heart rate variability (HRV); HRVLFn, normalized low-frequency components of HRV; n.u., normalized units.

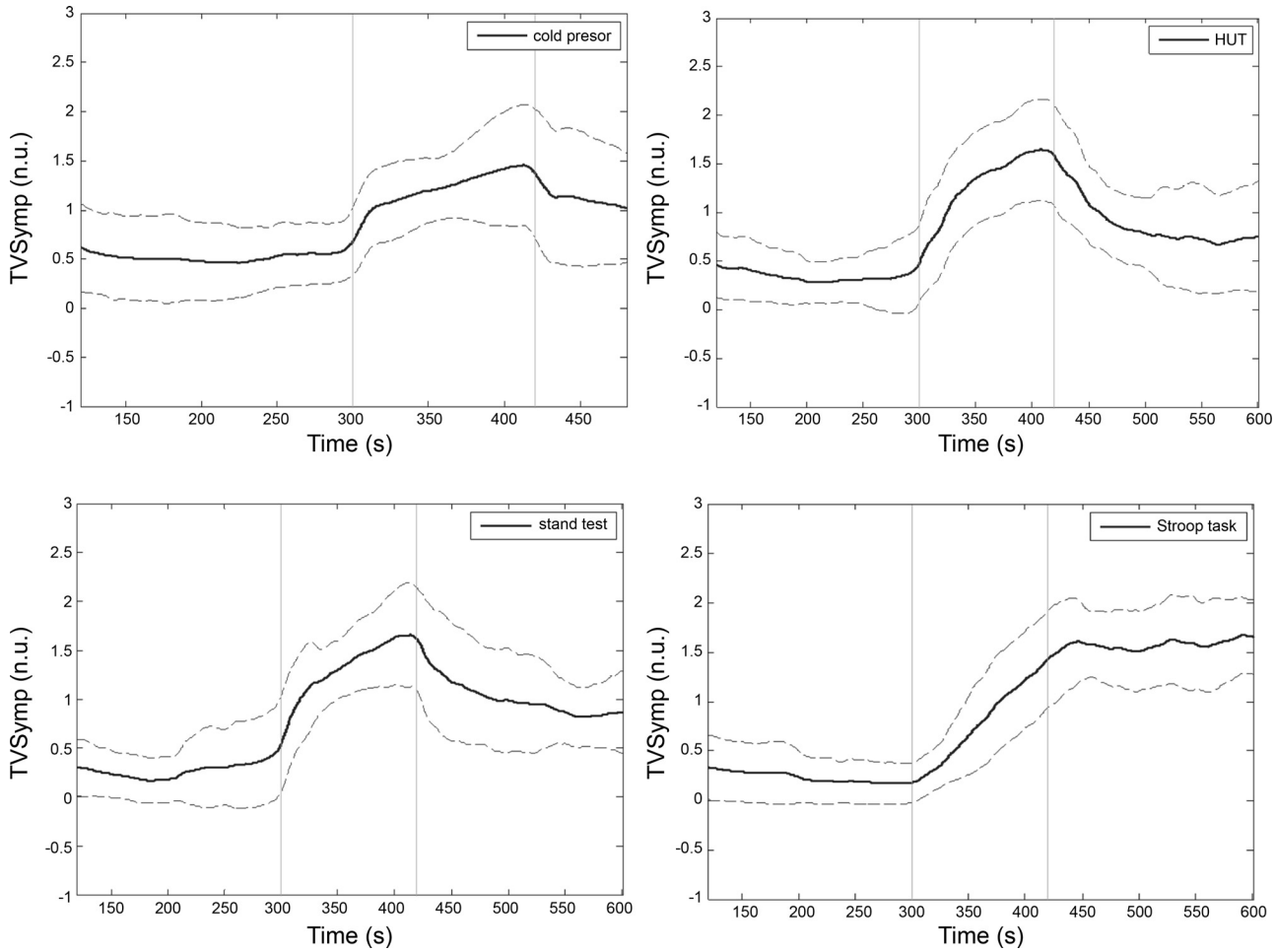

Fig. 4. Evolution (means ± SD) of TVSymp, Time-varying index of sympathetic tone, for the four tests: cold pressor, HUT (head-up tilt), stand test, and the Stroop task. TVSymp is at baseline levels before the test is performed.

renergic and ganglionic pharmacological blockade (14, 24, 28, 31), noradrenaline measurement in urine or plasma (15, 27, 32), microneurography (13, 56), plasma noradrenaline kinetics (4, 6), HRV analysis (1, 34, 54a), or imaging techniques (22). However, hemodynamic measurements and pharmacological blockade are invasive and present limited reproducibility. Noradrenaline measurement provides only a "static" picture of sympathetic function. Microneurography is the only method for directly and continuously recording efferent postganglionic muscle sympathetic nerve activity; however, it is an invasive technique. Imaging techniques, including positron emission tomography and single photon emission computed tomography scanning, have been applied to visualize the sympathetic innervation of human organs with good success, but neuroimaging techniques are costly and require specialized technical support.

HRV analysis has been widely employed because it is a low-cost noninvasive continuous method to evaluate cardiac sympathetic regulation. The low-frequency components of HRV (0.045–0.15 Hz) are commonly used as a marker of sympathetic control, even though such components are known to be influenced by both the sympathetic and para-

Table 3. *Sensitivity analysis of sympathetic indices*

	Cold Pressor			70° Head-up Tilt			Stand Test			Stroop Task		
Index	*J*	AUC	Acc	*J*	AUC	Acc	*J*	AUC	Acc	*J*	AUC	Acc
TVSymp	0.75	0.80	0.88	0.92	0.91	0.96	0.83	0.88	0.92	1.00	0.92	1.00
SCL	0.50	0.66	0.75	0.42	0.63	0.71	0.58	0.69	0.79	0.83	0.85	0.92
NS.SCR	0.33	0.61	0.67	0.50	0.73	0.75	0.83	0.87	0.92	0.92	0.92	0.96
EDASympn	0.58	0.70	0.79	0.50	0.66	0.75	0.50	0.63	0.75	0.42	0.69	0.71
HRVLF	0.25	0.42	0.63	0.38	0.59	0.69	0.75	0.80	0.88	0.50	0.55	0.75
HRVLFn	0.38	0.48	0.69	0.88	0.81	0.94	1.00	0.88	1.00	0.38	0.44	0.69

J is Youden's index, AUC is area under the ROC curve, Acc is accuracy. TVSymp, Time-varying index of sympathetic tone; SCL, skin conductance level; NS.SCRs, nonspecific skin conductance responses; EDASympn, normalized sympathetic component of the EDA; HRVLF, low-frequency components of HRV; HRVLFn, normalized low-frequency components of HRV.

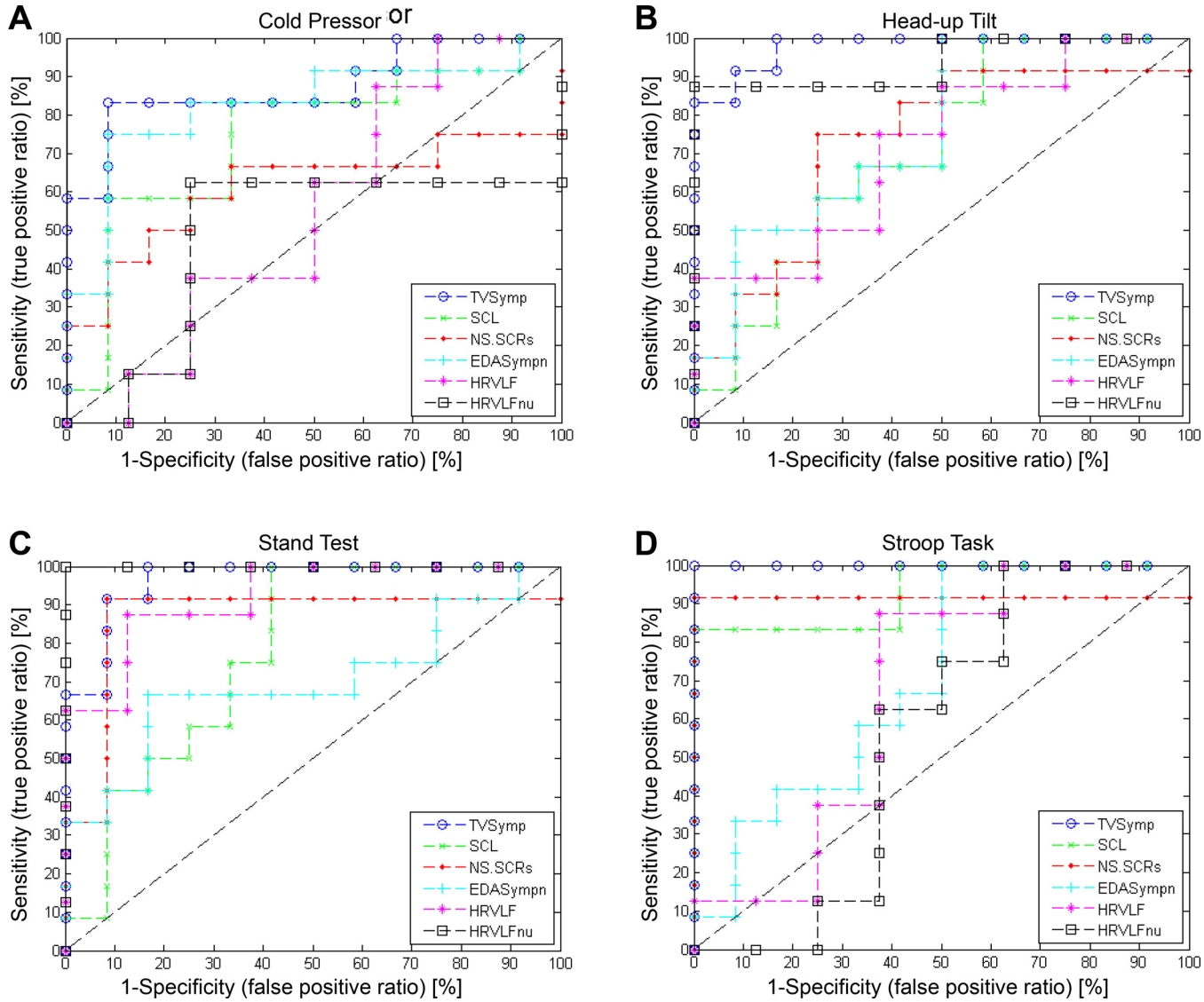

Fig. 5. Receiver operating characteristic (ROC) curves (sensitivity vs. 1-specificity) for the four tests: cold pressor (*A*), head-up tilt (*B*), stand test (*C*), and the Stroop task (*D*). The indices of sympathetic control are TVSymp, time-varying index of sympathetic tone; SCL, skin conductance level; NS.SCRs, nonspecific skin conductance responses; EDASympn, normalized sympathetic component of the EDA; HRVLF, low-frequency components of HRV; HRVLFn, normalized low-frequency components of HRV.

sympathetic nervous systems. Such influence reduces the accuracy of the technique. Time-domain analysis of EDA has also been used as a noninvasive marker of sympathetic nervous system regulation. The main advantage of EDA over HRV is that there is no parasympathetic innervation of eccrine sweat glands. However, a drawback to using time-domain measures of EDA is that they are highly variable between subjects (10).

A recent study suggests that sympathetic function influences the EDA spectrum mainly in the range of 0.045 to 0.25 Hz

Table 4. *Coefficient of variation and intra-class correlation results*

	Cold Pressor		70° Head-up Tilt		Stand Test		Stroop Task			
Indices	BL	Test	BL	Test	BL	Test	BL	Test	Average CV	Intra-Class Correlation (LB UB)
TVSymp	0.66	0.48	0.76	0.33	1.33	0.33	1.13	0.34	0.67	0.96 (0.9 0.99)
SCL	6.04	1.68	2.12	1.28	1.96	0.69	3.07	0.64	2.18	0.87 (0.67 0.97)
NS.SCR	1.09	0.91	1.50	0.76	1.11	0.48	1.56	0.40	0.98	0.92 (0.8 0.98)
EDASympn	0.68	0.47	0.90	0.45	0.59	0.48	0.72	0.37	0.58	0.81 (0.46 0.95)
HRVLF	0.90	0.69	0.82	1.32	1.02	0.91	0.85	0.69	0.90	0.84 (0.58 0.96)
HRVLFn	0.39	0.52	0.28	0.34	0.22	0.29	0.42	0.20	0.33	0.89 (0.72 0.97)

BL: baseline; LB and UB are upper and lower bounds, respectively, of the intra-class correlation with a level of significance of 0.05.

(43). This is in agreement with what we found, specifically, that the spectral amplitudes with frequencies of 0.08 to 0.24 Hz are the most responsive to sympathetic control, with the improvement in consistency and sensitivity shown by the time-frequency index, the TVSymp. We also performed VFCDM decomposition using sampling frequencies of 1 Hz and 0.8 Hz (not shown), to explore the effect of a higher-frequency resolution on the signal decomposition. This allowed us to compute the percentage of spectral power with higher spectral resolution and calculate the TVSymp index at frequencies between 0.04 and 0.08 Hz, which was part of the frequency-domain index in our previous study (43). Although this frequency band comprises about 10 to 15% of the total power, it was not as responsive to induced stimuli in this study, and its inclusion in computing the TVSymp resulted in lower sensitivity and performance of the index (assessed by signal detection theory). Performing time-invariant spectral density calculations on time-variant dynamics has been known to cause spectral distortion in the form of broadening of the spectral density (35); hence, we surmise that this may have caused the difference between the lower bound of the sympathetic dynamics found in this and our previous study (43). We believe that fs = 2 Hz is the most suitable sampling frequency and that the TVSymp index based on the frequency band 0.08 to 0.24 Hz is the most appropriate for capturing the sympathetic dynamics.

The responses of HRV dynamics and EDA to cold stress are also poorly understood; however, this stimulus has been increasingly used in clinical practice to evaluate autonomic function in cardiovascular regulation, because stressful cooling evokes an increase in sympathetic neurotransmissions via activation of cold thermoreceptors and nociceptors (46). HRVLF and HRVLFn are known to be insensitive detectors of stress induced by cold pressor, as various studies have reported increases (44, 48), decreases, or insignificant changes (11, 17, 33, 42). This is in agreement with our results, as HRVLF and HRVLFn exhibited no differences between baseline and the test for this stressor. Other studies found increases in SCL and NS.SCRs in healthy subjects when cold pressor was applied (40, 45). Despite the high variability (CV) for this test, we also found significant differences in NS.SCRs and SCL indices when comparing cold pressor to baseline. EDASympn index also exhibited sensitivity to this test, as reported previously (43). The time-frequency analysis index in this study, TVSymp, was able to discriminate between baseline and cold pressor. Indeed, although we observed that cold pressor was the most challenging test for detection, TVSymp performed the best among the various indices (highest J, AUC, and Acc).

HUT testing has been widely used to elicit sympathetic activation, as evidenced by increases in the low-frequency components of HRV, mainly in normalized units (9, 17, 21, 54). We were in agreement, as we found significant differences only in the normalized index, HRVLFn. EDA data during HUT are scarce, as only one study has tested skin conductance during HUT (37), showing an increase in the SCL in the tilt-negative group. In addition to the increase in SCL and NS.SCRs, the novel findings for the current study were the EDASympn and TVSymp responses, both of which have never been tested during HUT. EDASympn was able to discriminate between supine baseline and HUT, and TVSymp not only showed differences between baseline and HUT, but was the most sensitive, accurate, and responsive index at detecting when the subjects were under orthostatic stress induced by HUT.

Sympathetic tone normally increases with postural stimulation (e.g., stand test) (16, 60, 61). However, HRV has been shown to have poor reproducibility during an orthostatic challenge in healthy subjects, and even poorer reproducibility in a clinical population (49). In the supine position, HRVLF and HRVLFn were shown to have poor relative reliability (i.e., high intersubject variability). In this study, we found significant differences in both HRV indices during the stand test. Indeed, HRVLFn showed the highest performance in distinguishing between supine and standing position. For its part, EDA has not been used often for assessing the stress induced in a stand test (3, 43). In this study, we found significant differences in SCL and NS.SCRs between supine and standing. EDASympn, the time-invariant frequency-domain index, was also different between body postures, with a much lower variability than SCL and NS.SCRs. The time-frequency domain index, TVSymp, was significantly different between supine and upright positions. Even though the best detector for stand test was the HRVLFn, TVSymp exhibited a similarly good performance.

Low-frequency components of HRV have been shown to increase significantly during the Stroop task (12, 19, 58). We found that HRVLF, but not HRVLFn, significantly increased between baseline and the Stroop task. Regardless of their high variability during this test, SCL and NS.SCRs indices were significantly higher during the Stroop task compared with baseline. EDASymp also exhibited a significant increase. The performance and sensitivity of the TVSymp index was nearly perfect for the Stroop task. Beyond the significant differences encountered between baseline and the induced cognitive stress, TVSymp detected such stress with the maximum possible accuracy (Acc = 1) and performance ($J = 1$).

As shown in Table 2, the greatest change in the EDA indices to induced stimuli occurred for the Stroop task for TVSymp, SCL, and NS.SCR, which are then sequentially followed by stand and head-up tilt tests. For these three indices, the cold pressor stimuli induced the least change in their EDA responses. For HRVLF index, the greatest change was noted for the stand test followed by the Stroop task. While the EDASympn showed significant differences between the baseline and all stimuli, the induced changes in the amplitude of the EDA responses were similar for all tests. For TVSymp, SCL, and NS.SCR indices, the EDA responses are most sensitive to cognitive followed by orthostatic and cold pressor tests. However, further studies are needed to quantify and validate these findings using direct measures of the sympathetic activity.

The SCL index and NS.SCRs are consistent with sympathetic arousal, as they are elevated by administration of dextroamphetamine, caffeine, and threatening instructions (2, 63, 64). They also have relatively low within-subject variability (correlation of test-retest ranges from 0.50 to 0.70) but high variability between subjects (10). In this study, we also found SCL to be a sensitive, but very highly variable index. Although NS.SCRs are a consistent and fairly sensitive index, frequency-domain and time-frequency domain (EDASympn and TVSymp) indices do not rely on either manual or automatic SCR detection, which is usually more complex and time consuming. Because of its high sensitivity to four different types of stimuli and relatively low variability, the frequency-

domain EDASympn index was recognized as a promising index of sympathetic function under multiple stressors in healthy individuals. However, it lacks consistency between subjects and has an inability to detect postural stimulation (stand test) and cognitive stress, compared with SCL and NS.SCRs. TVSymp uses time-varying dynamics, an inherent characteristic of all biological systems; hence, it was shown to be a highly sensitive index of the sympathetic autonomic nervous system activity.

Conclusion

The TVSymp index is a suitable discriminator of the stress induced by cold pressor, HUT, stand test, and the Stroop task, and it has the potential to be used as a reliable marker of quantitative assessment of sympathetic function. Although HRVLFn was slightly more sensitive to postural stimulation from the stand test, it was not as sensitive to HUT, cold pressor, and the Stroop task compared with TVSymp. Overall, TVSymp was found to be more reliable and sensitive than indices based on low-frequency components of HRV, was highly consistent between subjects, and exhibited a lower variability compared with the time-domain measures of EDA. Finally, the frequency bands of the sympathetic nervous activities in healthy subjects can be defined to be most responsive in the frequencies between 0.08 and 0.24 Hz. More research is needed to determine whether these characteristics extend to patient populations.

Perspectives and Significance

Time-varying analysis of EDA not only overcomes the well-known lack of consistency of traditional time-domain analysis of EDA, it was also shown to be highly sensitive measure of the sympathetic dynamics. Moreover, time-varying analysis of EDA was found to be a more sensitive measure of the sympathetic dynamics than the low-frequency component of the heart rate variability. While this work explored cognitive, physical, and orthostatic stress, the time-varying analysis of EDA along with HRV could be extended to a host of other studies to better characterize and discriminate dynamics of the autonomic nervous system that may be indicative of impending fatigue and stress. An accurate understanding of the autonomic nervous system's dynamics pertaining to the situation at hand can lead to better guidance and interventions to improve human health and performance.

ACKNOWLEDGMENTS

This work was supported by the Office of Naval Research work unit N00014-15-1-2236.

DISCLOSURES

No conflicts of interest, financial or otherwise, are declared by the authors.

AUTHOR CONTRIBUTIONS

H.F.P.-Q. and K.H.C. conception and design of research; H.F.P.-Q. performed experiments; H.F.P.-Q. analyzed data; H.F.P.-Q., J.P.F., A.D.O.-C., and K.H.C. interpreted results of experiments; H.F.P.-Q. prepared figures; H.F.P.-Q. drafted manuscript; H.F.P.-Q., J.P.F., A.D.O.-C., and K.H.C. edited and revised manuscript; H.F.P.-Q., J.P.F., A.D.O.-C., and K.H.C. approved final version of manuscript.

REFERENCES

1. **Akselrod S, Gordon D, Madwed JB, Snidman NC, Shannon DC, Cohen RJ.** Hemodynamic regulation: investigation by spectral analysis. *Am J Physiol Heart Circ Physiol* 249: H867–H875, 1985.
2. **Bohlin G.** Delayed habituation of the electrodermal orienting response as a function of increased level of arousal. *Psychophysiology* 13: 345–351, 1976.
3. **Boucsein W, Fowles DC, Grimnes S, Ben-Shakhar G, roth WT, Dawson ME, Filion DL.** Society for Psychophysiological Research Ad Hoc Committee on Electrodermal Measures. Publication recommendations for electrodermal measurements. *Psychophysiology* 49: 1017–1034, 2012.
4. **Bradley T, Hjemdahl P.** Renal extraction of endogenous and radiolabelled catecholamines in the dog. *Acta Physiol Scand* 126: 505–510, 1986.
5. **Brod J, Fencl V, Hejl Z, Jirka J.** Circulatory changes underlying blood pressure elevation during acute emotional stress (mental arithmetic) in normotensive and hypertensive subjects. *Clin Sci* 18: 269–279, 1959.
6. **Brown GL, Gillespie JS.** The output of sympathetic transmitter from the spleen of the cat. *J Physiol* 138: 81–102, 1957.
7. **Chon KH, Dash S, Ju K.** Estimation of respiratory rate from photoplethysmogram data using time-frequency spectral estimation. *IEEE Trans Biomed Eng* 56: 2054–2063, 2009.
8. **Chon KH, Yang B, Posada-Quintero HF, Siu KL, Rolle M, Brink P, Birzgalis A, Moore LC.** A novel quantitative method for diabetic cardiac autonomic neuropathy assessment in type 1 diabetic mice. *J Diabetes Sci Technol* 8: 1157–1167, 2014.
9. **Cozza IC, Di Sacco THR, Mazon JH, Salgado MCO, Dutra SGV, Cesarino EJ, Souza HCD.** Physical exercise improves cardiac autonomic modulation in hypertensive patients independently of angiotensin-converting enzyme inhibitor treatment. *Hypertens Res* 35: 82–87, 2012.
10. **Crider A, Lunn R.** Electrodermal lability as a personality dimension. *J Exp Res Personal* 5: 145–150, 1971.
11. **DeBeck LD, Petersen SR, Jones KE, Stickland MK.** Heart rate variability and muscle sympathetic nerve activity response to acute stress: the effect of breathing. *Am J Physiol Regul Integr Comp Physiol* 299: R80–R91, 2010.
12. **Delaney JP, Brodie DA.** Effects of short-term psychological stress on the time and frequency domains of heart-rate variability. *Percept Mot Skills* 91: 515–524, 2000.
13. **Delius W, Hagbarth KE, Hongell A, Wallin BG.** General characteristics of sympathetic activity in human muscle nerves. *Acta Physiol Scand* 84: 65–81, 1972.
14. **Egan B, Panis R, Hinderliter A, Schork N, Julius S.** Mechanism of increased alpha adrenergic vasoconstriction in human essential hypertension. *J Clin Invest* 80: 812–817, 1987.
15. **Esler M, Jennings G, Korner P, Willett I, Dudley F, Hasking G, Anderson W, Lambert G.** Assessment of human sympathetic nervous system activity from measurements of norepinephrine turnover. *Hypertension* 11: 3–20, 1988.
16. **Ewing DJ, Clarke BF.** Diagnosis and management of diabetic autonomic neuropathy. *Br Med J* 285: 916–918, 1982.
17. **Florian JP, Simmons EE, Chon KH, Faes L, Shykoff BE.** Cardiovascular and autonomic responses to physiological stressors before and after six hours of water immersion. *J Appl Physiol (1985)* 115: 1275–1289, 2013.
18. **Freeman R, Chapleau MW.** Testing the autonomic nervous system. *Handb Clin Neurol* 115: 115–136, 2013.
19. **Garafova A, Penesova A, Cizmarova E, Marko A, Vlcek M, Jezova D.** Cardiovascular and sympathetic responses to a mental stress task in young patients with hypertension and/or obesity. *Physiol Res Acad Sci Bohemoslov* 63 *Suppl* 4: S459–S467, 2014.
20. **Gasquet H, Wootton AJ.** Variable-frequency complex demodulation technique for extracting amplitude and phase information. *Rev Sci Instrum* 68: 1111–1114, 1997.
21. **Gil E, Orini M, Bailon R, Vergara JM, Mainardi L, Laguna P.** Time-varying spectral analysis for comparison of HRV and PPG variability during tilt table test. *Conf Proc IEEE Eng Med Biol Soc* 2010: 3579–3582, 2010.
22. **Goldstein DS.** Clinical assessment of catecholaminergic function. *Stress, Catecholamines, and Cardiovascular Disease*. New York: Oxford University Press, 1995, p. 234–286.
23. **Grassi G, Esler M.** How to assess sympathetic activity in humans. *J Hypertens* 17: 719–734, 1999.

24. **Grassi G, Vailati S, Bertinieri G, Seravalle G, Stella ML, Dell'Oro R, Mancia G.** Heart rate as marker of sympathetic activity. *J Hypertens* 16: 1635–1639, 1998.
25. **Hanley JA, McNeil BJ.** The meaning and use of the area under a receiver operating characteristic (ROC) curve. *Radiology* 143: 29–36, 1982.
26. **Healey J, Picard RW.** Detecting stress during real-world driving tasks using physiological sensors. *IEEE Trans Intell Transp Syst* 6: 156–166, 2005.
27. **Hoeldtke RD, Cilmi KM, Reichard GA, Boden G, Owen OE.** Assessment of norepinephrine secretion and production. *J Lab Clin Med* 101: 772–782, 1983.
28. **Hollenberg NK, Adams DF, Solomon H, Chenitz WR, Burger BM, Abrams HL, Merrill JP.** Renal vascular tone in essential and secondary hypertension: hemodynamic and angiographic responses to vasodilators. *Medicine (Baltimore)* 54: 29–44, 1975.
29. **Huang NE, Shen Z, Long SR, Wu MC, Shih HH, Zheng Q, Yen NC, Tung CC, Liu HH.** The empirical mode decomposition and the Hilbert spectrum for nonlinear and non-stationary time series analysis. *Proc R Soc Lond Math Phys Eng Sci* 454: 903–995, 1998.
30. **Illigens BMW, Gibbons CH.** Sweat testing to evaluate autonomic function. *Clin Auton Res* 19: 79–87, 2009.
31. **Julius S, Pascual AV, London R.** Role of parasympathetic inhibition in the hyperkinetic type of borderline hypertension. *Circulation* 44: 413–418, 1971.
32. **Kopin IJ.** Catecholamine metabolism: basic aspects and clinical significance. *Pharmacol Rev* 37: 333–364, 1985.
33. **Liu YP, Lin YH, Chen YC, Lee PL, Tung CS.** Spectral analysis of cooling induced hemodynamic perturbations indicates involvement of sympathetic activation and nitric oxide production in rats. *Life Sci* 136: 19–27, 2015.
34. **Malliani A, Pagani M, Lombardi F, Cerutti S.** Cardiovascular neural regulation explored in the frequency domain. *Circulation* 84: 482–492, 1991.
35. **Marple SL.** *Digital Spectral Analysis: With Applications*. Englewood Cliffs, NJ: Prentice Hall, 1987.
36. **Mathias CJ, Bannister R.** Investigation of autonomic disorders [Online]. In: *Autonomic Failure: a Textbook of Clinical Disorders of the Autonomic Nervous System*, edited by Mathias CJ, Bannister R. Oxford, UK: Oxford University Press, p. 169–195. http://eprints.ucl.ac.uk/139822/ [Accessed Dec. 10, 2014].
37. **McGrady A, Kern-Buell C, Bush E, Khuder S, Grubb BP.** Psychological and physiological factors associated with tilt table testing for neurally mediated syncopal syndromes. *Pacing Clin Electrophysiol* 24: 296–301, 2001.
38. **McGraw KO, Wong SP.** Forming inferences about some intraclass correlation coefficients. *Psychol Methods* 1: 30, 1996.
39. **Metz CE.** Basic principles of ROC analysis. *Semin Nucl Med* 8: 283–298, 1978.
40. **Mezzacappa ES, Kelsey RM, Katkin ES.** Breast feeding, bottle feeding, and maternal autonomic responses to stress. *J Psychosom Res* 58: 351–365, 2005.
41. **Monti A, Médigue C, Mangin L.** Instantaneous parameter estimation in cardiovascular time series by harmonic and time-frequency analysis. *IEEE Trans Biomed Eng* 49: 1547–1556, 2002.
42. **Moses ZB, Luecken LJ, Eason JC.** Measuring task-related changes in heart rate variability. *Conf Proc IEEE Eng Med Biol Soc* 2007: 644–647, 2007.
43. **Posada-Quintero HF, Florian JP, Orjuela-Cañón AD, Aljama-Corrales T, Charleston-Villalobos S, Chon KH.** Power spectral density analysis of electrodermal activity for sympathetic function assessment. *Ann Biomed Eng* (April 8, 2016). doi: 10.1007/s10439-016-1606-6.
44. **Prakash ES, Madanmohan Sethuraman KR, Narayan SK.** Cardiovascular autonomic regulation in subjects with normal blood pressure, high-normal blood pressure and recent-onset hypertension. *Clin Exp Pharmacol Physiol* 32: 488–494, 2005.
45. **Prystav GH.** Electrodermal, cardiac, and respiratory activity to repeated cold pressor stimulation in drug addicts. *J Gen Psychol* 94: 259–270, 1976.
46. **Robertson D, Johnson GA, Robertson RM, Nies AS, Shand DG, Oates JA.** Comparative assessment of stimuli that release neuronal and adrenomedullary catecholamines in man. *Circulation* 59: 637–643, 1979.
47. **Rouleau JL, Moyé LA, de Champlain J, Klein M, Bichet D, Packer M, Dagenais G, Sussex B, Arnold JM, Sestier F.** Activation of neurohumoral systems following acute myocardial infarction. *Am J Cardiol* 68: 80D–86D, 1991.
48. **Sanchez-Gonzalez MA, May RW, Koutnik AP, Kabbaj M, Fincham FD.** Sympathetic vasomotor tone is associated with depressive symptoms in young females: a potential link between depression and cardiovascular disease. *Am J Hypertens* 26: 1389–1397, 2013.
49. **Sandercock GRH, Bromley PD, Brodie DA.** The reliability of short-term measurements of heart rate variability. *Int J Cardiol* 103: 238–247, 2005.
49a. **Schwartz PJ, La Rovere MT, Vanoli E.** Assessment: Clinical autonomic testing report of the Therapeutics and Technology Assessment Subcommittee of the American Academy of Neurology. *Neurology* 46: 873–880, 1996..
50. **Setz C, Arnrich B, Schumm J, La Marca R, Tröster G, Ehlert U.** Discriminating stress from cognitive load using a wearable EDA device. *IEEE Trans Inf Technol Biomed* 14: 410–417, 2010.
51. **Siu KL, Sung B, Cupples WA, Moore LC, Chon KH.** Detection of low-frequency oscillations in renal blood flow. *Am J Physiol Renal Physiol* 297: F155–F162, 2009.
52. **Spallone V, Morganti R, Fedele T, D'Amato C, Maiello MR.** Reappraisal of the diagnostic role of orthostatic hypotension in diabetes. *Clin Auton Res* 19: 58–64, 2009.
53. **Stroop RJ.** Studies of interference in serial verbal reactions. *J Exp Psychol* 18: 643–662, 1935.
54. **Takimoto Y, Yoshiuchi K, Ishizawa T, Yamamoto Y, Akabayashi A.** Autonomic dysfunction responses to head-up tilt in anorexia nervosa. *Clin Auton Res* 24: 175–181, 2014.
54a. **Task Force of the European Society of Cardiology and the North American Society of Pacing and Electrophysiology.** Heart rate variability: Standards of measurement, physiological interpretation, and clinical use. *Eur Heart J* 17: 354–381, 1996.
55. **Thomas CB, Stanley JA, Kendrick MA.** Observations on some possible precursors of essential hypertension and coronary artery disease. VII. The subjective reaction to the cold pressor test as expressed in the verbal response. *J Chronic Dis* 14: 355–365, 1961.
56. **Vallbo AB, Hagbarth KE, Torebjörk HE, Wallin BG.** Somatosensory, proprioceptive, and sympathetic activity in human peripheral nerves. *Physiol Rev* 59: 919–957, 1979.
57. **Vidaurre C, Sander TH, Schlögl A.** BioSig: the free and open source software library for biomedical signal processing. *Comput Intell Neurosci* 2011: 935364, 2011.
58. **Visnovcova Z, Mestanik M, Javorka M, Mokra D, Gala M, Jurko A, Calkovska A, Tonhajzerova I.** Complexity and time asymmetry of heart rate variability are altered in acute mental stress. *Physiol Meas* 35: 1319–1334, 2014.
59. **Wang H, Siu K, Ju K, Chon KH.** A high resolution approach to estimating time-frequency spectra and their amplitudes. *Ann Biomed Eng* 34: 326–338, 2006.
60. **Wieling W, van Brederode JF, de Rijk LG, Borst C, Dunning AJ.** Reflex control of heart rate in normal subjects in relation to age: a data base for cardiac vagal neuropathy. *Diabetologia* 22: 163–166, 1982.
61. **Williamson JW, McColl R, Mathews D.** Evidence for central command activation of the human insular cortex during exercise. *J Appl Physiol (1985)* 94: 1726–1734, 2003.
62. **Youden WJ.** Index for rating diagnostic tests. *Cancer* 3: 32–35, 1950.
63. **Zahn TP, Rapoport JL, Thompson CL.** Autonomic effects of dextroamphetamine in normal men: implications for hyperactivity and schizophrenia. *Psychiatry Res* 4: 39–47, 1981.
64. **Zhong Y, Bai Y, Yang B, Ju K, Shin K, Lee M, Jan KM, Chon KH.** Autonomic nervous nonlinear interactions lead to frequency modulation between low- and high-frequency bands of the heart rate variability spectrum. *Am J Physiol Regul Integr Comp Physiol* 293: R1961–R1968, 2007.
65. **Zhong Y, Jan KM, Chon KH.** Frequency modulation between low- and high-frequency components of the heart rate variability spectrum may indicate sympathetic-parasympathetic nonlinear interactions. *Conf Proc IEEE Eng Med Biol Soc* 1: 6438–6441, 2006.